Available online at www.sciencedirect.com
ScienceDirect
International Journal of Pharmaceutics 344 (2007) 128–134
INTERNATIONAL JOURNAL OF PHARMACEUTICS
www.elsevier.com/locate/ijpharm

Potentialities of silica/alginate nanoparticles as Hybrid Magnetic Carriers

Michel Boissière [a], Joachim Allouche [a], Corinne Chanéac [a], Roberta Brayner [b], Jean-Marie Devoisselle [c], Jacques Livage [a], Thibaud Coradin [a,*]

[a] *Chimie de la Matière Condensée de Paris (CMCP), CNRS-UMR 7574, Université Pierre et Marie Curie, 4 Place Jussieu, 75252 Paris Cedex 05, France*
[b] *Interfaces, Traitements, Organisation et Dynamique des Systèmes (ITODYS), CNRS-UMR 7086, Université Denis Diderot, 2 Place Jussieu, 75251 Paris Cedex 05, France*
[c] *Laboratoire de Matériaux Catalytiques et Catalyse en Chimie Organique (LMCCCO), CNRS-UMR 5618-ENSCM-UMI, Institut Fédératif Charles Gerhardt, 8 rue de l'Ecole Normale, 34296 Montpellier Cedex 5, France*

Received 16 February 2007; received in revised form 21 May 2007; accepted 23 May 2007
Available online 31 May 2007

Abstract

The possibility to associate traditional bio-organic capsules, such as polymer nanoparticles or liposomes, with silica has been recently demonstrated, opening the route to the design of novel nanocomposites that exhibit promising properties as drug carriers. In this context, we describe here the elaboration of silica/alginate nanoparticles incorporating magnetic iron oxide colloids and fluorescent carboxy-fluoroscein. These nanocomposites were characterized by electron microscopy, X-ray diffraction and magnetic measurements. The release of the fluorophore was investigated in vitro and was demonstrated to occur in 3T3 fibroblast cells. Further grafting of organic moieties on particle surface is also described. These data suggest that hybrid nanoparticles are flexible platforms for the developments of multi-functional bio-capsules.

Keywords: Alginate; Silica; Maghemite; Hybrid materials; Nanoparticles

1. Introduction

The so-called sol–gel process is a method allowing the room temperature synthesis of many inorganic materials, such as ceramics and glasses (Brinker and Scherrer, 1990). It relies on an inorganic polymerization reaction starting from molecular precursors. This reaction can take place in a wide range of experimental conditions, including aqueous solutions and neutral pH that are therefore compatible with the presence of organic and biological molecules (Avnir et al., 2006). Even whole cells can now be maintained alive over several weeks in silica gels (Nassif et al., 2002).

Applications of the sol–gel process in medicinal science include the elaboration of diagnostic tools, bone repair materials and artificial organs (Coradin et al., 2006a). In the field of drug release systems, silica-based materials were evaluated both *in vitro* and *in vivo* as gels (Sieminska and Zerda, 1996; Nicoll et al., 1997; Ahola et al., 2000), microspheres (Kortueso et al., 2000) and nanoparticles (Lai et al., 2003; Barbé et al., 2004).

When compared to traditional polymeric carriers, silica-based nanoparticles may present several advantages. They exhibit enhanced and controllable mechanical and chemical stability. Their porosity can also be easily tailored in terms of pore size and organization. Finally, the chemistry of silica surface modification by covalent grafting of organic moieties has been widely studied. All these properties suggest the sol–gel process of silica should allow the design of materials with tunable release profiles and surface properties.

However, at this time, data on silica nanoparticles toxicity are scarce. On the one hand, colloidal silica was shown to induce red blood cells hemolysis (Gerashchenko et al., 2002) and blood monocytes injuring (Pomeroy and Filice, 1988). On the other hand, surface-modified silica nanoparticles were successfully used for *in vivo* gene therapy (Bharali et al., 2005). Additionally, nothing is known about the possible *in vivo* degradation of these particles and the toxicity of the resulting products.

An intermediate alternative between polymer and silica nanoparticles lies in the design of organic–inorganic hybrid carriers (Coradin et al., 2006b). The underlying concept is to select

* Corresponding author. Tel.: +33 144275517; fax: +33 144274769.
E-mail address: coradin@ccr.jussieu.fr (T. Coradin).

0378-5173/$ – see front matter © 2007 Elsevier B.V. All rights reserved.
doi:10.1016/j.ijpharm.2007.05.055

suitable nanomaterials among the large diversity of bio-organic nanoparticles developed in pharmaceutical science over the last 30 years (Couvreur and Vauthier, 2006) and to combine them with silica obtained via the sol–gel process. At this time, two different approaches were explored along this line. The first one consists in the elaboration of silica-coated liposomes, termed liposils (Bégu et al., 2003). It was shown that the integrity of the phospholipid vesicles was preserved within the hybrid capsule (Bégu et al., 2004). A second approach involves the deposition of silica on biopolymer capsules. This process was described as biomimetic since it was inspired from the natural processes of silica formation found in some micro-organisms (Lopez et al., 2005). The feasibility of this strategy was first demonstrated on alginate and gelatine macrospheres (Coradin et al., 2001; Coradin and Livage, 2005a) and was then extended to micro- and nanoparticles for both biopolymers (Boissière et al., 2006; Allouche et al., 2006). These hybrid nanoparticles showed enhanced thermal stability when compared to their biopolymer equivalents. Moreover, they could be up-taken by fibroblast cells and degraded intra-cellularly, without inducing rapid cell death.

Based on these data, it was recently proposed that these biopolymer/silica nanoparticles could serve as platforms for the design of multi-functional bio-capsules, called Hybrid Magnetic Carriers (HYMAC) (Boissière et al., in press). These nanocomposites would consist of hybrid particles incorporating magnetic colloids and drugs, that would be surface-modified by biocompatible polymers (such as poly-ethyleneglycol) and/or specific signal biomolecules, for the design of magnetically modulated therapeutic systems (Häfeli, 2004; Gupta and Gupta, 2005).

First steps in that direction were performed through the design of iron oxide/silica/alginate nanocapsules using a spray-drying technology (Boissière et al., in press). However, it was found that magnetite nanocrystals used as magnetic colloids were unstable during the process, leading to the release of Fe^{2+} ions and formation of lepidocrocite Fe(OOH) and fayalite Fe_2SiO_4 nanoparticles.

In this work, we wish to report our attempts to further evaluate the suitability of these magnetic nanoparticles as drug carriers. To overcome the problem of magnetite unstability, maghemite nanocrystals were evaluated as suitable magnetic colloids to form HYMAC nanocomposites. Carboxyfluorosceine was selected as a model molecule to investigate the particle release behavior both in simulated biological conditions and within fibroblast cells. The possibility to modify the particle surface with organic moieties was also studied.

2. Materials and methods

2.1. Nanoparticles preparation

Magnetite Fe_3O_4 colloids were prepared following a previously described procedure based on the precipitation of solutions of $FeCl_2$ (2 M, 20 mL) and $FeCl_3$ (1 M, 80 mL) in ammonia (Jolivet et al., 2004). The solution was centrifuged and washed with deionized water until the washing water reach a neutral pH. The resulting suspension of surface-oxidized magnetite colloids was left to settle overnight so that only the smallest particles remain in the supernatant solution. To obtain fully oxidized maghemite γ-Fe_2O_3 colloids, the thus-obtained magnetite particles were suspended in perchloric acid $HClO_4$ for 30 min. Analyses of the supernatant by inductively coupling plasma-atomic emission spectroscopy (ICP-AES) indicate a concentration of 30 ± 5 mM in iron.

For the maghemite/silica/alginate nanocomposite preparation, 100 mL of an alginate (alginic acid sodium salt from *Macrocystis pyrifera*, low viscosity, Sigma) aqueous solution (0.05 wt.%), 10 mL of the maghemite supernatant solution, 80 mL of water and 10 mL of diluted sodium silicate solution (0.1 M) were successively introduced in a 250 mL flask under stirring. In order to study the release properties of the hybrid nanoparticles, 200 μl of a 0.1 wt.% aqueous solution of carboxyfluoroscein (CF), selected as a model hydrophilic drug, was also added in the initial solution. The resulting mixture was sonicated for 5 min before introduction in the spray-dryer. Details about the aerosol apparatus and spray-drying procedure can be found elsewhere (Boissière et al., in press).

2.2. Nanoparticles characterization

Transmission electron microscopy (TEM) of particles directly deposited on carbon-coated copper grid was performed on a JEOL 100 CX microscope working at 120 kV.

Thermogravimetric analyses (TGA/DTG) were performed on a NETZSCH TG 209 equipment in the 30–800 °C temperature range with a 10 °C min^{-1} heating step.

X-ray energy dispersive spectrometry (EDX) was performed using an (EDXD) EDAX system equipped with a super ultra thin window (SUTW) connected to a JEOL JSM 6100 scanning electron microscope. In order to obtain reliable data on the carbon content of the materials, measurements were performed at 3 kV on uncoated samples deposited, and not glued, on the sample holder. Atomic compositions (%), obtained with Genesis software from 3 different measurements, are given within a ±5% error.

Nanocomposites were investigated by powder X-Ray diffraction (XRD). The diffractograms were recorded on a Panalytical diffractometer using the Co Kα radiation in the reflection mode, between 10° and 80° in 2θ (step = 0.05; accumulation delay = 30 s). The nature of the iron oxide phase was obtained by comparison with corresponding JCPDS files.

Magnetic measurements were performed using a Quantum Design MPMS-5S SQUID magnetometer in the temperature range 2–300 K.

2.3. In vitro release study

In vitro release studies were conducted in a flow-through dissolution cell (12-mm diameter, USP apparatus 4, Sotax, Switzerland; the norm chosen was USP 28-NF-23 (2005)) which was a dissolution testing unit for solid dosage form, using the USP/EP flow-through method (Bhattachar et al., 2002).

The flow-through cell dissolution used in the experiments may be described as having three parts: the lower cone, the middle cylindrical portion and a filter head on top (Fig. 1a)

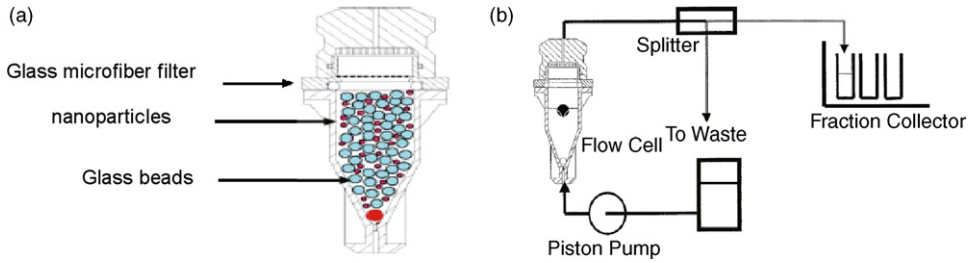

Fig. 1. Schematic drawing of (a) the 12 mm flow-through cell containing nanoparticles and glass beads and (b) corresponding open system.

(Charnay et al., 2004). The dissolution medium enters the cone through a capillary bore situated on the bottom and flows upwards. The cone is separated from the cylindrical portion and a glass microfiber filter. The powder was loaded into the flow-through cell on the bottom of the cylindrical portion. The glass beads also provided laminar flow and decreased the dead volume within the flow through cells. It was determined that the ratio of nanoparticles-to-glass beads should not be too high, or back-pressure problems might result. Therefore, 50 mg of nanoparticles and 10 g of glass beads were selected for use in 12-mm cells. As back-pressure problems may also arise due to inappropriate selection of filters, a fiberglass filter (0.45 μm) was selected for the nanoparticles systems reported here. The flow rate of the dissolution medium (phosphate buffer solution (PBS), pH 7.4) across the cell is set at 6.5 mL/min and the cell is thermostated at 37 °C. This system can be operated in open system configuration where media flows through the cell containing the drug product to a fraction collector (Fig. 2b). Each fraction was analysed with a UV-visible spectrophotometer in order to monitor the OD variation at $\lambda = 430$ nm during the release process. Experiments were performed in triplicate.

2.4. Cell uptake experiments

The 3T3 fibroblast cells were cultured onto glass coverslips in Dulbecco's modified Eagle's medium (DMEM) containing 10% fetal bovine serum (FBS) and pen/strep (penicillin/streptomycin) at 37 °C in 5% CO_2 and 95% air. After 24 h, cells were incubated with 200 mg of capsules for 24 h at 37 °C in the same medium. After this delay, the suspensions were removed and washed three times with PBS. The last step consists in fixing the cells with 4% para-formaldehyde (PFA). The cellular uptake efficiency of particles was determined by fluorescence microscopic images. The excitation wavelength and emission wavelength was 460 and 515 nm, respectively, for carboxy-fluoroscein.

2.5. Nanoparticle surface modification

2.5.1. Gold-coated nanoparticle

Two hundred milligrams of nanoparticles were dispersed in anhydrous toluene and 5 drops of mercaptopropyltriethoxysilane (MPTS, Sigma) was poured in the suspension. Reaction was left to occur 2 h under magnetic stirring before filtering, washing five times with toluene and drying in air. An Au colloidal solution was prepared by a simple method based on reduction of gold salt (Turkevich et al., 1951). Fifty milligrams of $HAuCl_4$ were dissolved in 500 mL of deionised water. The solution was heated at 80 °C and 0.5 g of trisodium citrate was added. After 1 h30 stirring at 80 °C, the colour of the solution turned from transparent yellow to red, indicating the reduction of Au^{3+} to Au^0. Finally, the suspension was left to cool at room temperature. The MPTS-

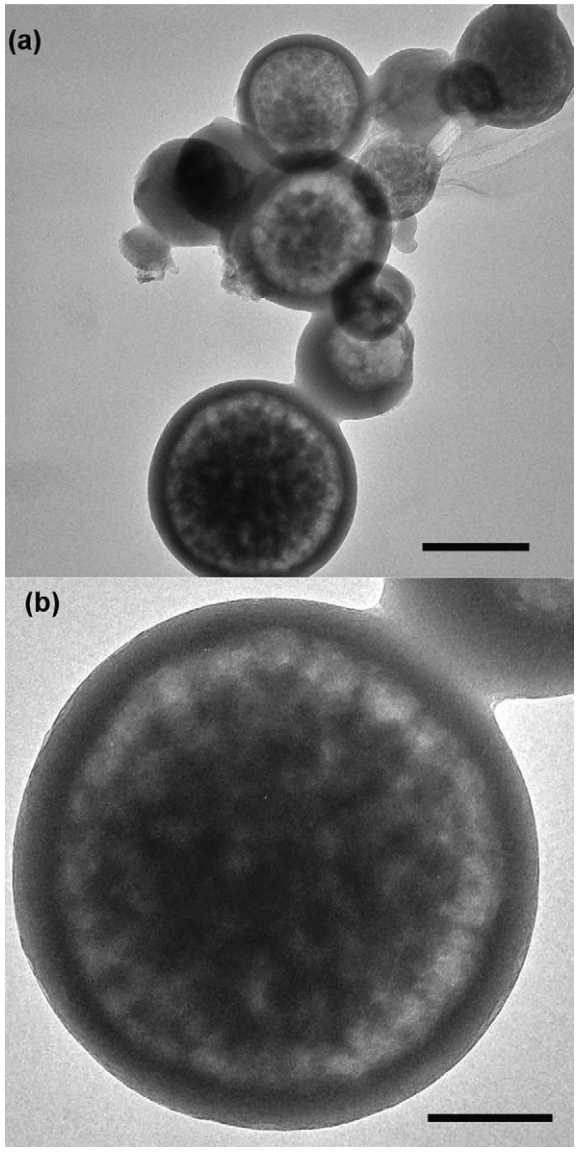

Fig. 2. Transmission electron micrographs of nanoparticles (scale bar: (a) 100 nm, (b) 50 nm)).

modified nanoparticles were dispersed in 10 mL of ethanol and 3 mL of Au metallic colloidal solution were added and left to react for 1 h. The resulting nanocomposites were recovered by filtration, washed five times with ethanol and drying in air.

2.5.2. PEG-coated nanoparticles

The PEG-bearing organosilane PEGME-IPTES was synthesized by the reaction of 3-(triethoxysilyl)propyl isocyanate (IPTES, Aldrich) with poly(ethylene glycol) methyl ether (PEGME, $M_w \approx 2000\ g\ mol^{-1}$, Aldrich) in the presence of dibutyltin laurate, following a literature procedure (Oh et al., 2005). Five hundred milligrams of nanoparticles were suspended in toluene (10 mL) and the mixture was sonicated for 5 min. Three grams of PEGME-IPTES were then added and the reaction left to proceed for 2 h. The resulting nanoparticles were recovered by centrifugation, washed with ethanol and dried in air.

3. Results and discussion

3.1. Nanoparticles preparation and characterization

The aerosol sample was recovered as a pinkish powder that was studied by TEM. The size of the particles was found in the 50–200 nm range, in good agreement with previous data (Fig. 2a). However, these particles exhibit a core–shell structure consisting of a 10–20 nm dense outer layer encapsulating a complex mixture of an electron-transparent matrix, that may correspond to the alginate network, and of darker nanoparticles, that are consistent with iron oxide colloids incorporation (Fig. 2b).

The organic (alginate + CF) content of the hybrid capsules, determined by TGA/DTG analysis, is ca. 30 wt% (Fig. 3). From DTG, it was possible to identify the thermal degradation of CF close to 225 °C, corresponding to a 0.5 wt% weight loss, followed by alginate decomposition in the 240–500 °C region, corresponding to a 29 wt.% loss. Such an CF:alginate weight ratio of ca. 0.02 should be only considered as an approximate value due to the error range of TGA measurements but appears in good agreement with the initial content of the spray-dried solution. The carbon:silicon:iron relative content was determined by EDX to be 65:33:2 in atomic percent (not shown). EDX is a surface analysis technique and is therefore more sensitive to the elements located in the shell of the nanoparticles. As TEM micrographs suggest that maghemite colloids are mostly concentrated within the nanoparticle core, the measured iron content is probably under-estimated.

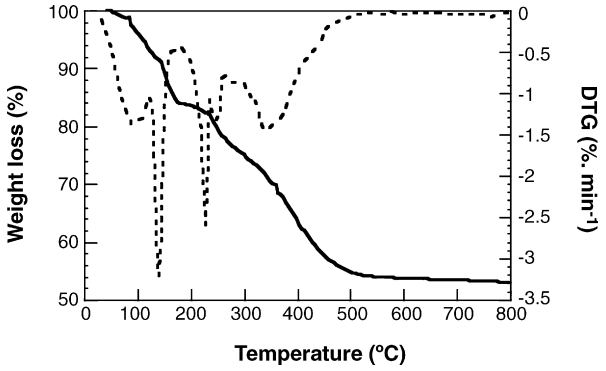

Fig. 3. TGA curve (plain line) and DTG (dashed line) of nanoparticles.

The incorporation of iron oxide colloids was confirmed by XRD and magnetic measurements (not shown). Main diffraction peaks corresponded to the maghemite γ-Fe_2O_3 but the formation of lepidocrocite Fe(OOH) could also be observed. The features of zero-field-cooling/field cooling (ZFC/FC) susceptibility curves of these samples indicate a superparamagnetic behaviour with blocking temperature $T_B \approx 100$ K. A hysteresis loop could be recorded at 2 K, indicating that the sample is ferromagnetic at this temperature, with corresponding coercitivity value $H_c = 830$ Oe.

Comparison of these results with our previous data provides some interesting insights. The two procedures only differ from the nature of magnetic colloids as magnetite Fe_3O_4 was previously used instead of maghemite γ-Fe_2O_3 and the addition of carboxy-fluoroscein in the present work. However, such differences have a significant impact on the resulting nanoparticles. If no variation in nanocomposite particle size is observed, their internal structure is significantly different as a core–shell organization is obtained here in contrast to the homogeneous alginate/silica network observed in the previous work. One explanation would lie in the possibility of interactions between CF and silicates via hydrogen bonding of the fluorophore hydroxyl groups and the silanol Si-OH functions. Alternatively, iron oxide nanoparticle surfaces have a good affinity for carboxylate-bearing organic molecules. Indeed, both effects may be involved here but it is difficult, at this time, to provide a precise mechanism for the core–shell structure formation.

In addition, the use of maghemite instead of magnetite limits the surface destabilization of the magnetic colloids, and corresponding Fe^{2+} surface desorption, during the spray-drying process, as indicated by the absence of iron silicate phases previously observed (Boissière et al., in press). However, formation of lepidocrocite Fe(OOH) is still taking place, indicating that further efforts will have be made to insure magnetic colloid integrity during the aerosol processing. Finally, a comparison of magnetic data indicate that introduction of maghemite colloids leads to a decrease in blocking temperature and increase in coercitivity when compared to magnetite-based nanoparticles, that may be attributed to a difference in colloid aggregation within the hybrid network.

3.2. Release studies

The release profile of CF initially encapsulated in iron oxide/alginate/silica nanoparticles at neutral pH is shown on Fig. 4. It is characterized by a rapid fluorophore diffusion over the first 10 min leading to 80% cumulative release, followed by a slower liberation reaching about 90% after 4 h. In the absence of silica, alginate-based nanoparticles were found to dissolve in less than 5 min, indicating a stabilizing effect of the mineral component.

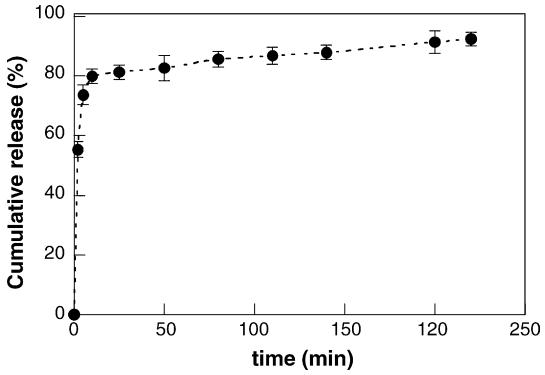

Fig. 4. Release profile of carboxy-fluoroscein in a flow-through dissolution cell (errors bars correspond to standard deviation).

Previous reports have shown that in vitro silica gel degradation occurs via an erosion mechanism (Ahola et al., 2000). This mechanism implies the hydrolysis of Si–O–Si siloxane bonds that is usually observed when silica gels are placed in an excess of water (Iler, 1979). It can therefore be suggested that the CF release first occurs through the degradation of the nanoparticle outer shell that is expected to be very fast due to its small thickness (10–20 nm). In a second step, the degradation of the nanoparticle core is expected to occur via the dissolution of the alginate network (Boissière et al., 2006). Such a degradation may not result in the complete dissolution of the material but rather in the formation of iron oxide–alginate–silica aggregates. The elimination of intravenous alginate through urine excretion (Hagen et al., 1996) and the degradation of iron oxide nanoparticles by liver cells (Briley-Saebo et al., 2004) were already demonstrated. Therefore, the only origin for possible toxicity of nanocomposite degradation by-products concerns the silica component. As mentioned earlier, not enough in vivo data are available at this time to evaluate the associated toxicity that may in addition strongly depends on the form (molecular, colloidal) and size of silica species.

The CF release within 3T3 fibroblast cells was also investigated by optical fluorescence microscopy. On Fig. 5, after 24 h of contact, fluorescent particles can be located within the cells, confirming nanocomposite intra-cellular incorporation. Moreover, a more diffuse fluorescence is visible all over the cytoplasm, suggesting that CF has been released after particles internalization. Although no further attempts were made to assess nanoparticle toxicity, we observed that after 24 h, fibroblasts cells were

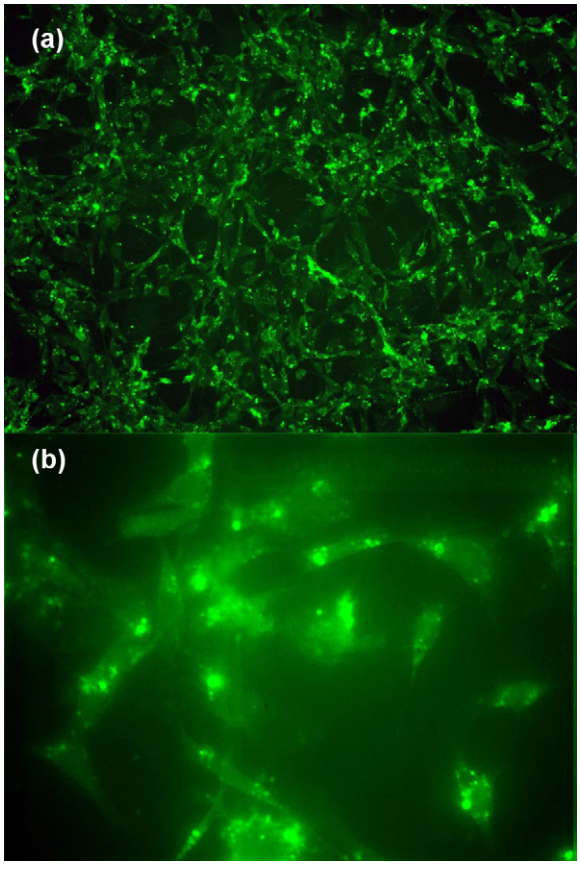

Fig. 5. Optical fluorescence micrographs of 3T3 fibroblasts cells after 24 h contact with CF-loaded nanoparticles ((a) ×40; (b) ×100).

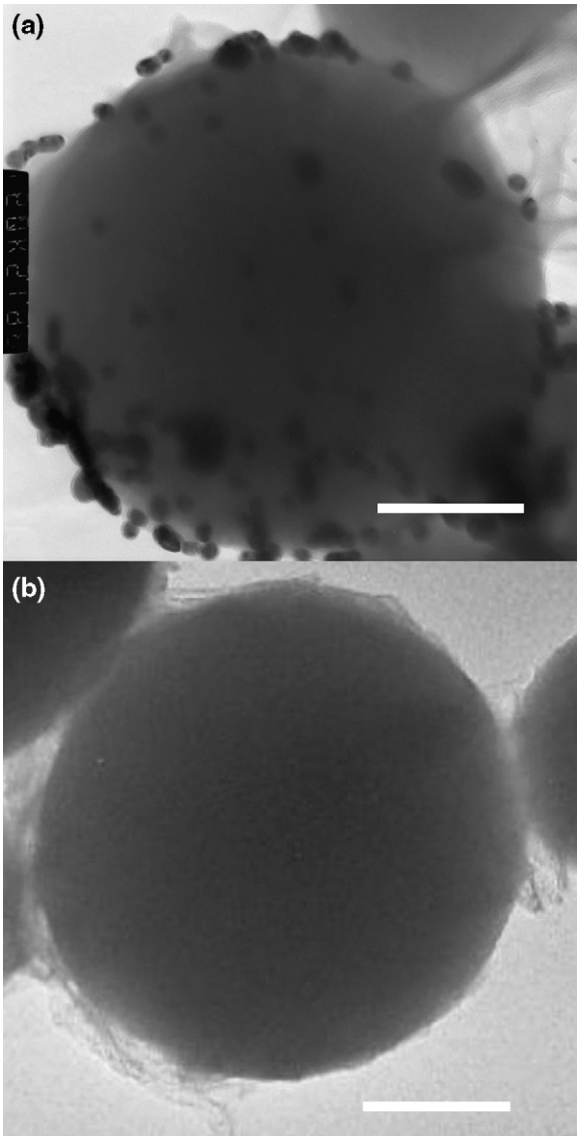

Fig. 6. Transmission electron micrographs of (a) gold-decorated nanoparticle and (b) PEG-coated nanoparticle (scale bar: 50 nm).

still adhering on the glass substrate, a good indication of maintained viability. These results are in good agreement with the previously demonstrated possibility for these cells to incorporate hybrid nanoparticles and to degrade them intra-cellularly, without rapid loss of viability (Allouche et al., 2006; Boissière et al., 2006, in press).

3.3. Nanoparticle surface modification

In a step forward, we have evaluated the suitability of the hybrid nanoparticles for surface grafting of organic moieties, in the perspective of designing of long-circulating carriers with targeting properties (Brigger et al., 2002).

CF-containing iron oxide/alginate/silica nanoparticles were therefore reacted with mercaptopropyltrietoxysilane (MPTS). In these conditions, the silanol groups of MPTS are expected to interact with Si-OH groups of the particle surface, leading to covalent binding of the thiol-bearing chain. The presence of S atom could be detected by EDX but was more easily visualized by addition of gold colloids that are known to present a very good affinity for –SH groups. Resulting particles are shown on Fig. 6a, demonstrating the deposition of Au colloids on the nanoparticle surface. The presence of Au was also confirmed by EDX giving a Si:Au relative amount of 90:10 in atomic percent. It was checked that no gold is present on the hybrid nanoparticle surface in the absence of MPTS grafting.

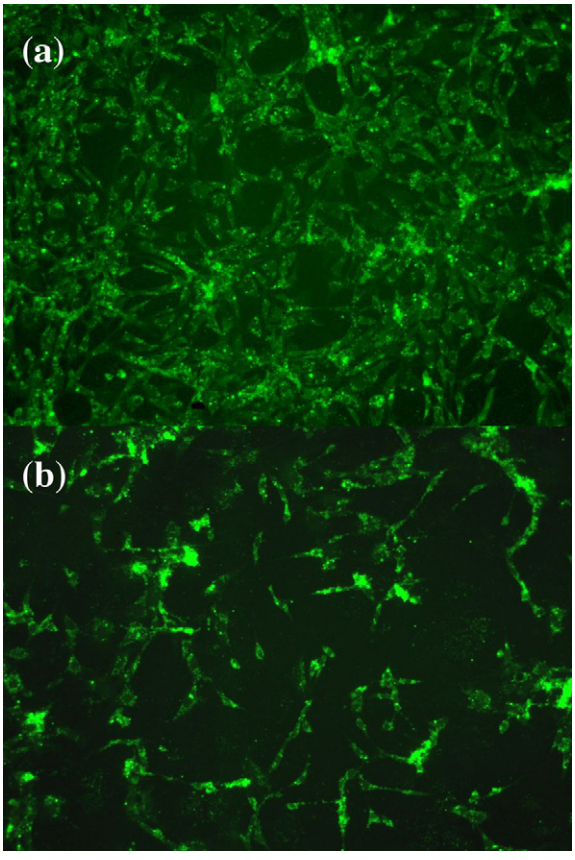

Fig. 7. Optical fluorescence micrographs of 3T3 fibroblasts cells after 24 h contact with (a) gold-coated and (b) PEG-coated CF-loaded nanoparticles (×40).

PEG-coated nanoparticles were also synthesized via covalent grafting of the PEGME-IPTES precursor. Resulting particles appear surrounded by thin veil-like network, are shown on Fig. 6b, suggesting the successful deposition of the polymer.

Optical fluorescence microscopy imaging of fibroblast cells after 24 h contact with these gold-coated nanoparticles (Fig. 7a) were very similar to those obtained for non-coated nanocomposites, This indicates that the presence of gold colloids do not interfere significantly with the nanoparticle uptake and CF intra-cellular release. In contrast, for PEG-coated nanoparticles, a significant decrease in fluorescence intensity was observed, with some particle aggregates being visible outside the cells. These observations suggest that the nanoparticle incorporation is hindered by the presence of PEG. It is well-known that most endocytic pathways are mediated by proteins, such as clathrin (Gonzalez-Gaitan and Stenmark, 2003). As poly-(ethylene glycol) is known to limit protein adsorption, it can be suggested that its presence on the nanoparticle surface interferes with the endocytic process.

4. Conclusion

This study aimed at validating our concept of hybrid biopolymer-silica capsules incorporating magnetic colloids as drug carriers. Our results indicate that:

(i) A better preservation of the magnetic colloids within the silica/alginate hybrid nanoparticles is possible using maghemite instead of magnetite colloids.
(ii) Drug-like molecules can be incorporated in and released from these magnetic nanoparticles. In the conditions of this work, the presence of carboxy-fluoroscein leads to the formation of core–shell systems whose degradation results in a two-step release process.
(iii) The surface modification of the nanoparticles by gold colloids or by PEG chains is possible. Note that although gold colloids were used in this work as indicators for thiol function grafting, they also exhibit some interesting properties as cytochemical markers (Horisberger, 1981). Moreover, the presence of PEG influences nanoparticle internalization by fibroblast cells, providing some preliminary information on the endocytic process.

The successful incorporation of magnetic colloids in polymer-based nanoparticles has already been widely described and used for Magnetic Resonance (MR) imaging, hyperthermia therapy and magnetic drug targeting (Weissleder et al., 1995). In first two fields of applications, the advantage of using hybrid nanoparticles is not straightforward. In contrast, drug delivery systems require an elaborate control of carrier degradation and surface chemistry and our results suggest that our HYMAC nanoparticles may significantly contribute to this field. In the present work, we show that the presence of silica decreases the kinetics of degradation of the alginate nanoparticles. It may be suggested that a modification of the initial alginate:silicate ratio may allow a better tuning of this degradation process. Moreover, our data indicate that the encapsulation of a different drug (or

surrogate) would lead to a different structure of the nanocomposites. For instance, cationic molecules are known to interact strongly with silicates and may result in the precipitation of silica within the alginate network, as already demonstrated for gelatin (Coradin et al., 2005). In parallel, the low affinity of silicates for hydrophobic substrates should lead to phase separation phenomena so that the resulting structure may consist of two non-interpenetrating polymer/silica networks (Brinker and Scherrer, 1990). Therefore our approach is very flexible in terms of design of nanoparticles with different architectures and hence different release profiles. In addition, our successful attempts to modify the hybrid nanoparticle surface strengthen our previous assumption that the presence of silica shifts the surface modification chemistry of these systems from polymer- to inorganic-based process and hence to the widely developed bio-functionalization procedures of silica substrates by organosilanes.

These three main aspects (role of the silicate:alginate ratio, influence of the encapsulated drug, surface bio-functionalization) are currently under study, together with further investigations of the nanoparticle internalization process and intra-cellular degradation.

References

Ahola, M., Kortueso, P., Kangasniemi, I., Kiesvaara, J., Yli-Urpo, A., 2000. Silica xerogel carrier material for controlled release of toremifene citrate. Int. J. Pharm. 195, 219–227.

Allouche, J., Boissière, M., Hélary, C., Livage, J., Coradin, T., 2006. Biomimetic core–shell gelatine/silica nanoparticles: a new example of biopolymer-based nanocomposites. J. Mater. Chem. 16, 3121–3126.

Avnir, D., Coradin, T., Lev, O., Livage, J., 2006. Recent bio-applications of sol–gel materials. J. Mater. Chem. 16, 1013–1030.

Bhattachar, S.N., Wesley, J.A., Fioritto, A., Martin, P.J., Babu, S.R., 2002. Dissolution testing of a poorly soluble compound using the flow-through cell dissolution apparatus. Int. J. Pharm. 236, 135–143.

Bharali, D.J., Klejbor, I., Stachowiak, E.K., Dutta, P., Roy, I., Kaur, N., et al., 2005. Organically modified silica nanoparticles: a nonviral vector for in vivo gene delivery and expression in the brain. Proc. Natl. Acad. Sci. U.S.A. 102, 11539–11544.

Barbé, C., Bartlett, J., Kong, L., Finnie, K., Lin, H.Q., Larkin, M., et al., 2004. Silica particles: a novel drug-delivery system. Adv. Mater. 16, 1959–1966.

Bégu, S., Durand, R., Lerner, D.A., Charnay, C., Tourné-Péteilh, C., Devoisselle, J.M., et al., 2004. Preparation and characterization of siliceous material using liposomes as template. Chem. Commun., 640–641.

Bégu, S., Girod, S., Lerner, D.A., Jardiller, N., Tourné-Péteilh, C., Devoisselle, J.M., et al., 2003. Characterization of a phospholipid bilayer entrapped into non-porous silica nanospheres. J. Mater. Chem. 14, 1316–1320.

Boissière, M., Meadows, P.J., Brayner, R., Hélary, C., Livage, J., Coradin, T., et al., 2006. Turning biopolymer particles into hybrid capsules: the example of silica/alginate nanocomposites. J. Mater. Chem. 16, 1178–1182.

Boissière, M., Allouche, J., Brayner, R., Chanéac, C., Livage, J., Coradin, T. Design of iron oxide/silica/alginate Hybrid Magnetic Carriers (HYMAC). J. Nanosci. Nanotechnol., in press.

Brigger, I., Dubernet, C., Couvreur, P., 2002. Nanoparticles in cancer therapy and diagnosis. Adv. Drug. Deliv. Rev. 54, 631–651.

Briley-Saebo, K., Bjornerud, A., Grant, D., Ahlstrom, H., Berg, T., Kindberg, G.M., et al., 2004. Hepatic cellular distribution and degradation of iron oxide nanoparticles following intravenous injection in rats: implications for magnetic resonance imaging. Cell Tissue Res. 316, 315–323.

Brinker, C.J., Scherrer, G., 1990. Sol–Gel Science. The Physics and Chemistry of Sol–Gel Processing. Academic, Boston.

Charnay, C., Begu, S., Tourne-Peteilh, C., Nicole, L., Lerner, D.A., Devoisselle, J.M., et al., 2004. Inclusion of ibuprofen in mesoporous templated silica: drug loading and release property. Eur. J. Pharm. Biopharm. 57, 533–540.

Coradin, T., Mercey, E., Lisnard, L., Livage, J., 2001. Design of silica-coated microcapsules for bioencapsulation. Chem. Commun., 2496.

Coradin, T., Livage, J., 2005a. Synthesis, characterization and diffusion properties of biomimetic silica-coated gelatine beads. Mater. Sci. Eng. C 25, 201–205.

Coradin, T., Bah, S., Livage, J., 2005. Gelatine/silicate interactions: from nanoparticles to composite gels. Colloids Surf. B 35, 53–58.

Coradin, T., Boissière, M., Livage, J., 2006a. Sol–gel chemistry in medicinal science. Curr. Med. Chem. 13, 99–108.

Coradin, T., Allouche, J., Boissière, M., Livage, J., 2006b. Sol–gel biopolymer/silica nanocomposites in biotechnology. Curr. Nanosci. 2, 219–230.

Couvreur, P., Vauthier, C., 2006. Nanotechnology: intelligent design to treat complex disease. Pharm. Res. 23, 1417–1450.

Gerashchenko, B.I., Gun'ko, V.M., Gerashchenko, I.I., Mironyuk, I.F., Leboda, R., Hosoya, H., et al., 2002. Probing the silica surfaces by red blood cells. Cytometry 49, 56–61.

Gonzalez-Gaitan, M., Stenmark, H., 2003. Endocytosis and signaling: a relationship under development. Cell 115, 513–521.

Gupta, A.K., Gupta, M., 2005. Synthesis and surface engineering of iron oxide nanoparticles for biomedical applications. Biomaterials 26, 3995–4021.

Hagen, A., Skjak-Braek, G., Dornish, M., 1996. Phrmacokinetics of sodium alginate in mice. Eur. J. Pharm. Sci. 4, 100–101.

Häfeli, U.O., 2004. Magnetically modulated therapeutic systems. Int. J. Pharm. 277, 19–24.

Horisberger, M., 1981. Colloidal gold: a cytochemical marker for light and fluorescence microscopy and for Transmission and Scanning Electron Microscopy. Scan. Electron. Microsc. 2, 9–31.

Iler, R.K., 1979. The Chemistry of Silica. Wiley-Interscience, New York.

Jolivet, J.P., Chanéac, C., Tronc, E., 2004. Iron oxide chemistry. From molecular clusters to extended solid network. Chem. Commun., 477–483.

Kortueso, P., Ahola, M., Kangas, M., Kangasniemi, I., Yli-Urpo, A., Kiesvaara, J., et al., 2000. In vitro evaluation of sol–gel processed spray dried silica gel microspheres as carrier in controlled drug delivery. Int. J. Pharm. 200, 223–229.

Lai, C.Y., Trewyn, B.G., Jeftinija, D.M., Jeftinija, K., Xu, S., Jeftinija, S., et al., 2003. A mesoporous silica nanosphere-based carrier system with chemically removable CdS nanoparticle caps for stimuli-responsive controlled release of neurotransmitters and drug molecules. J. Am. Chem. Soc. 125, 4451–4459.

Lopez, P.J., Gautier, C., Livage, J., Coradin, T., 2005. Mimicking biogenic silica nanostructures formation. Curr. Nanosci. 1, 73–83.

Nassif, N., Bouvet, O., Rager, M.-N., Roux, C., Coradin, T., Livage, J., et al., 2002. Living bacteria in silica gels. Nat. Mater. 1, 42–44.

Nicoll, S.B., Radin, S., Santos, E.M., Tuan, R.S., Ducheyne, P., 1997. In vitro release kinetics of biologically active transforming growth factor-β1 from a novel porous glass carrier. Biomaterials 18, 853–859.

Oh, C., Ki, C.D., Chang, J.Y., Oh, S.-G., 2005. Preparation of PEG-grafted silica particles using emulsion method. Mater. Lett. 59, 929–933.

Pomeroy, C., Filice, G.A., 1988. Effect of intravenous silica on the course of *Nocardia asteroids* pneumonia. Inf. Immun. 56, 2507–2511.

Sieminska, L., Zerda, T.W., 1996. Diffusion of steroids from sol–gel glass. J. Phys. Chem. 100, 4591–4597.

Turkevich, J., Stevenson, P.C., Hillier, J., 1951. A study of the nucleation and growth processes in colloidal gold. Discuss. Faraday. Soc. 11, 55–75.

Weissleder, R., Bodanov, A., Neuwelt, E.A., Papisov, M., 1995. Long-circulating iron oxides for MR imaging. Adv. Drug Deliv. Rev. 16, 321–334.